

AREA OF THE UNSTABLE SOLUTION OF ROLLING EQUATION – JUMPS OF THE OSCILLATIONS AMPLITUDE

Wojciech Wawrzyński

Gdynia Maritime University
Faculty of Navigation, Department of Ship Operation
Jana Pawła II Av. 3, 81-345 Gdynia, Poland
tel.: +48 58 6201301
e-mail: w.wawrzynski@wn.am.gdynia.pl

Abstract

The most interesting motion of the ship is rolling. This is because the rolling amplitudes are much bigger than amplitudes of other degrees of freedom and under resonance conditions, which can exceed 40°. In such a case, when the maximum of the righting arm curve is placed at relatively small angles, the roll equation reveals a strongly nonlinear character and bistability areas as well as an area of unstable solutions of the roll equation occurs. Together with the appearance of the above-mentioned areas, amplitude jumps are possible. In the study, the case of strongly nonlinear rolling is analysed. For the purpose of numerical simulations, the 1DOF mathematical model of rolling with damping dependent on amplitude and frequency is used. The article presents the roll spectrum including the bistability areas and the area of unstable solutions for one loading condition of the offshore support vessel. It is demonstrated that for strongly nonlinear rolling, rolling with two different amplitudes for the same value of excitation is possible. It is also shown that transitions (jumps) between these amplitudes are possible too. A few scenarios of jumps of the rolling amplitude within the region of unstable solutions of the rolling equation are presented. The presented rolling scenarios show that under some circumstances rolling can be observed as chaotic.

Keywords: ship rolling, nonlinear oscillations, nonlinear resonance, bistability, bifurcations, amplitude jumps

1. Introduction

Ship motions are defined by six degrees of freedom. However, the most interesting motion of a ship is rolling. The reasons are the values of oscillations amplitudes, which can be achieved. The amplitude of rolling frequently exceeds angles of 20-25° and in resonance conditions even 40°. In comparison, amplitudes of pitch motion do not exceed 1-2°. Additionally, for medium and especially large amplitudes of rolling, in many cases a mathematical model of rolling reveals nonlinear behaviour.

Generally, a mathematical model of rolling is the nonlinear dynamical system, which is described by the second-order nonlinear ordinary differential equation. A parameter that determines the nonlinearity of rolling most of all is the restoring moment, which is commonly, described by the righting arms curve (*GZ* curve). Usually, for small amplitudes, the nonlinearity of the *GZ* curve is small and can be ignored. In such a case, the mathematical model with linear restoring moment works quite well. However when medium and especially large amplitudes of rolling are analysed then phenomena typical for nonlinear oscillations should be considered. In rolling, these phenomena are most often revealed when the maximum of the *GZ* curve is located at relatively small angles – for an intact ship, it concerns angles close to 30°. Therefore, given that extreme amplitudes of rolling in resonance conditions can achieve 35-40° it should be assumed that the phenomena typical for nonlinear oscillations could occur under real conditions.

Obviously, couplings with other degrees of freedom as well as the nonlinearity of roll damping or nonlinearity of the moment of added mass due to water dragging by the rolling hull can have an impact on the nonlinearity of oscillations. However, the influence of the last two is weak and can

be clearly seen in the range of small and medium amplitudes and only in cases when the restoring moment is close to linear.

The characteristic phenomena for nonlinear oscillations are:

- the resonance frequency dependence on rolling amplitude [2, 4, 12],
- bistability (multivaluedness) – the possibility of rolling with two different amplitudes for the same value of the excitation moment [4, 18],
- bifurcation – phenomenon which refers to the sudden qualitative change in the solution of the mathematical model due to a small smooth change made to the value of some parameter – the bifurcation [3, 4, 10],
- jumps of rolling amplitude – since two different amplitudes of rolling are possible, the transitions (jumps) between them are possible too [4, 7, 12].

Some of the above-mentioned phenomena are related directly to the area of the unstable solutions, which can be observed inside the area of the possible solutions of the rolling equation, when strong nonlinearity occurs. To reveal the area of unstable solutions the standard roll spectrum is insufficient. The roll spectrum should be developed with the use of a two-dimensional analysis. This analysis is performed for the assumed surface of the excitation-frequency values in combination with external perturbations taking the form of an impact with a variable value of the force [12].

The goal of the research was an analysis of the possible scenarios of amplitude jumps in the range of frequencies of the unstable solution of rolling equation. However, due to the limited size of this article, only a few scenarios are presented and discussed.

2. Applied model of ship rolling

Since the phenomena characteristic for nonlinear oscillations are mainly the derivative of the restoring moment nonlinearity and a general analysis is made then the use of the 1-DOF system is most convenient.

For the constant value of roll, damping the general form of the 1-DOF model of rolling can be presented in the form:

$$(I_x + A_{44})\ddot{\phi} + B_e\dot{\phi} + K(\phi) = M_w(t) \cdot \cos(\omega_e t) + M_d(t), \quad (1)$$

where I_x denotes the transverse moment of ship's inertia, A_{44} is the moment of added mass due to water dragging by the rolling hull, B_e is the equivalent linear roll damping coefficient, $K(\phi)$ describes the restoring moment of the ship, M_w is the exciting moment, M_d is the additional external moment, ω_e is the encounter frequency of waves and t denotes time. The moments M_w and M_d are time dependent. In case of M_w , this allows for periodic changes in the value of roll excitation, so groups of higher and lower waves can be simulated. The time-varying external moment M_d can be used to simulate short external excitation impulses (e.g. caused by the wind).

After a few transformations, the roll equation (1) becomes:

$$\ddot{\phi} + 2\mu \cdot \dot{\phi} + \frac{g}{r_x^2} GZ(\phi) = \xi_w(t) \cdot \cos(\omega_e t) + \xi_d(t), \quad (2)$$

where μ is the damping coefficient, g is the gravity acceleration, r_x is the gyration radius of a ship and added masses (which is assumed to be constant for the purpose of this study), GZ is the righting arm, ξ_w is the exciting moment coefficient, and ξ_d is the coefficient of the additional external moment.

For the purpose of the research, which is discussed the restoring moment, was approximated by the ninth order polynomial with odd powers only:

$$GZ(\phi) = C_1 \cdot \phi + C_3 \cdot \phi^3 + C_5 \cdot \phi^5 + C_7 \cdot \phi^7 + C_9 \cdot \phi^9, \quad (3)$$

where C_1 to C_9 are the coefficients obtained with the use of the least squares method.

To take into account the damping dependence on amplitude of rolling, the damping term in the equation (2) has been modified to the form given by Himeno [5]. As a result, it becomes:

$$\ddot{\phi} + 2\alpha \cdot \dot{\phi} + \beta \cdot \dot{\phi}|\dot{\phi}| + \gamma \cdot \phi^3 + \frac{g}{r_x^2} GZ(\phi) = \xi_w \cdot \cos(\omega_e t) + \xi_d(t), \quad (4)$$

where α , β and γ are coefficients, which have been calculated analytically according to a simple Ikeda's method [8] with one modification – the bilge keel component was calculated according to the full Ikeda's method [6]. This modification was made due to the inconsistency in the results for the bilge keel component calculated according to the full and simplified method.

When the surface of damping coefficients for the considered range of amplitudes and frequencies of rolling was obtained, then for the constant values of roll frequency, the coefficients α , β and γ were fitted fulfilling the condition (5) for a full spectrum of considered amplitudes. However, when the frequency spectrum is too wide, the method gives some inaccuracy.

$$\mu(\phi_\alpha, \omega) = \alpha + \frac{4}{3\pi} \phi_\alpha \omega \beta + \frac{3}{8} \phi_\alpha^2 \omega^2 \gamma. \quad (5)$$

The last step was performed so that the coefficients α , β and γ take rolling frequency into account – the series of each coefficient (calculated for successive frequencies) has been individually fitted for the 4th order polynomial with roll frequency as an argument:

$$\alpha(\omega) = a_\alpha + b_\alpha \omega + c_\alpha \omega^2 + d_\alpha \omega^3 + e_\alpha \omega^4, \quad (6)$$

$$\beta(\omega) = a_\beta + b_\beta \omega + c_\beta \omega^2 + d_\beta \omega^3 + e_\beta \omega^4, \quad (7)$$

$$\gamma(\omega) = a_\gamma + b_\gamma \omega + c_\gamma \omega^2 + d_\gamma \omega^3 + e_\gamma \omega^4. \quad (8)$$

The final form of the roll equation with damping dependence on amplitude and frequency is obtained:

$$\ddot{\phi} + 2\alpha(\omega_e) \cdot \dot{\phi} + \beta(\omega_e) \cdot \dot{\phi}|\dot{\phi}| + \gamma(\omega_e) \cdot \phi^3 + \frac{g}{r_x^2} GZ(\phi) = \xi_w \cdot \cos(\omega_e t) + \xi_d(t). \quad (9)$$

It should be noted that the Ikeda's method is fully applicable for amplitudes not bigger than 0.4 rad and does not consider changes to roll damping due to bilge keel emergence and deck submergence. For the latter problem, no exact analytical method is known at the moment – some propositions of a solution can be found in [1].

3. Roll spectrum for the strongly nonlinear system

When rolling is strongly nonlinear, the standard roll spectrum is insufficient to describe the possible behaviour of a ship. For the strongly nonlinear system, the roll spectrum should be developed with the use of a two-dimensional analysis [12]. The result of such calculations for the offshore support vessel ($T = 6.10$ m, $GM_0 = 2.50$ m), performed using the equation (9) for the assumed and widespread surface of excitation-frequency values combined with external perturbations in the form of an impact with a variable value of the force is presented in Fig. 1. The calculations were performed with the use of the equation (9), where the surface of the damping coefficients, estimated according to the simple Ikeda's method is shown in Fig. 2.

The parts of Fig. 1 are described below, however it should be noted that the meaning of the terms *area* and *region* differs; the term *area* is used concerning a separate part of the graph whereas the term *region* refers to the frequency range.

- Point **P** – the bistability origin point – the onset point of bistability areas **C** and **D**,
- Areas **C** and **D** – rolling bistability areas. In area **C**, the oscillations are non-resonant, but the energy provided by the excitation moment is big enough for resonant oscillations within the area **D**. The transitions between the non-resonant and resonant oscillations and so between **C** and **D** areas are possible. The lower limit of the area **C** (dashed line) determines the minimum value of the energy (excitation moment) needed for resonant oscillations,

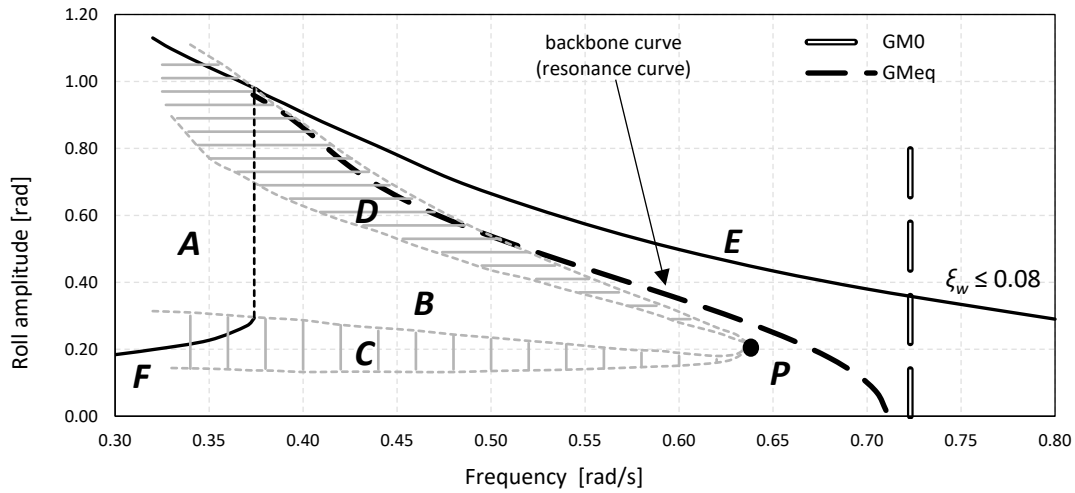


Fig. 1. Roll spectrum and bistability areas for the offshore support vessel ($T = 6.10$ m, $GM_0 = 2.50$ m, the GZ curve is softening spring), determined for the excitation coefficient $\xi_w \leq 0.08$ and the damping dependent on rolling amplitude and frequency

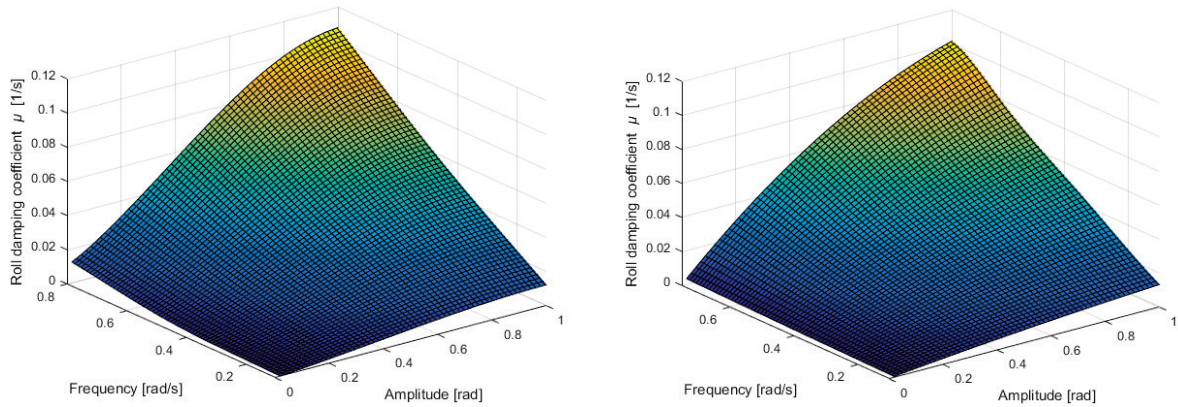


Fig. 2. Damping coefficients for the offshore support vessel ($T = 6.10$ m, $GM_0 = 2.50$ m, $C_B = 0.778$, $C_M = 0.987$, bilge keel: $l_{BK} = 19.00$ m, $b_{BK} = 0.30$ m) calculated according to the simple Ikeda's method (left drawing) and next approximated using coefficients $\alpha(\omega)$, $\beta(\omega)$ and $\gamma(\omega)$ in equation (9) (right drawing)

- Areas **B** and **A** – areas of unstable solution of the rolling equation. Areas **B** and **A** appear together with the bistability areas **C** and **D** and are separated at the frequency of the bifurcation with jump up (in Fig. 1 dashed vertical line between areas **B** and **A**). The location of this separation line depends on the value of the excitation moment assumed to determine the roll spectrum. When the bistability areas **C** and **D** are not expanded enough, area **A** does not appear. The entire border of the area of unstable solutions of the rolling equation is the line of bifurcation. However, it needs to be highlighted that to determine the lower border of area **A**, calculations using values of the excitation moment bigger than those assumed to determine the roll spectrum are necessary. Additionally, for the case presented in Fig. 1 the left border of area **A** was not designated because of the inaccuracy of the GZ curve approximation for angles over 1.1 rad for the loading condition, which was studied.

More complex description of the roll spectrum in the form as in Fig. 1 can be found in [12].

4. Rolling amplitude jumps within the region of unstable solution of the rolling equation

In this section the roll equation (9) behaviour within region **B** and **A** is described and a few possible scenarios of these areas crossing are presented. The presented scenarios were confirmed by rolling numerical simulations performed for the OSV vessel. Most of the presented simulations

were conducted for frequency $\omega = 0.5$ rad/s, where lower and upper limits of bistability areas, in radians, are: **C**(0.135; 0.235) and **D**(0.436; 0.539).

Generally, two types of scenarios of amplitude jumps can be distinguished. The first one refers to situations when the frequency or value of the exciting moment M_w is changed. In such a case, when the solution of the equation (9) enters the unstable area then the transition (amplitude jump) occurs. In Fig. 3 (left), initially a ship is rolling with an amplitude on the upper limit of the area **C**. From the 380 second of simulation time the value of M_w is increased only by 1%. As an effect, the transition (amplitude jump) to the area of resonant oscillations can be observed. In Fig. 3 (right), initially a ship is rolling with an amplitude on the lower limit of area **D**. From the 1000 second of simulation time the value of M_w is decreased by 1% and the transition (amplitude jump) to the non-resonant oscillations occurs. Further, entering area **B** at the lower limit causes a jump not to the upper limit of area **B** but the upper limit of area **D**, while entering area **B** at the upper limit causes a jump not to the lower limit of area **B** but the lower limit of area **C**.

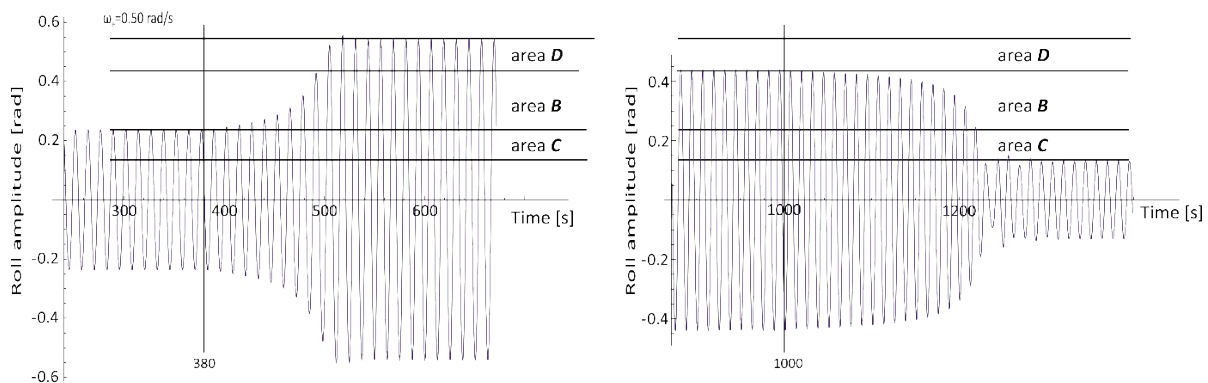


Fig. 3. Roll time history for the OSV vessel ($T=6.10$ m, $GM_0=2.50$ m). Transitions between the bistability areas cause by very small and smooth change) in value of the exciting moment (change by 1% of its initial value)

The second scenario refers to situations when the frequency and value of excitation moment are constant in time but due to e.g. wind or couplings, some additional impulses occurring for a short time period. For this second scenario, two cases are described below:

Cases when the excitation moment induces a stable amplitude of rolling below the lower limit of the bistability area C

In Fig. 4, the initial and stable roll amplitude is below the lower limit of area **C**. From 380 second of simulation time the additional excitation moment M_d is introduced. Its value and duration time are enough to force crossing of area **C** and area **B** and entering area **D** – resonance-rolling area. At 440-second moment M_d is stopped and although the oscillations are inside the resonance area the amplitude is decreasing to its initial value – the energy provided by the excitation moment is too small to maintain such a large rolling amplitude, independently from resonance conditions.

Crossing area **C** as well area **B** requires providing a sufficient amount of additional energy, despite the fact that area **B** is the area of unstable solution of rolling equation. Quantity of the energy needed for a transition to area **D** depends on the initial rolling amplitude (transition distance) and on damping value. When value of M_d is large then its time of duration can be short. For smaller values of M_d longer time of duration is indispensable. If this additional energy supply will be stopped before achieving the area of resonance conditions, the solution quickly returns to the initial value of amplitude (Fig. 5). However, when the resonance area is achieved then the return to the initial value of rolling amplitude takes much more time (this time depends on the depth of entry into the area **D**) and oscillations with large amplitudes are significantly more numerous (Fig. 4).

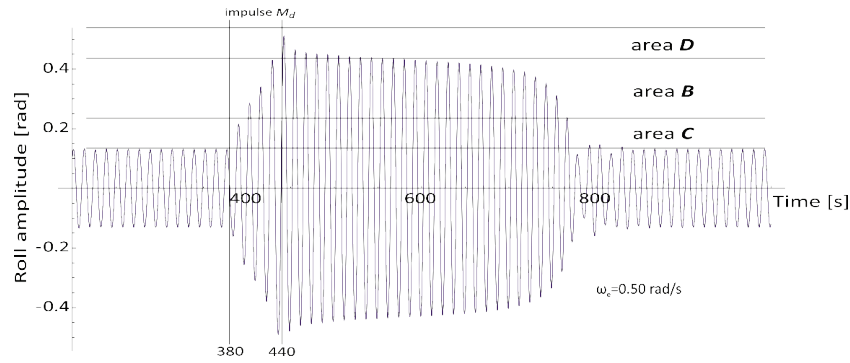


Fig. 4. Roll time history for the OSV vessel ($T = 6.10$ m, $GM_0 = 2.50$ m, $\zeta_w = 0.039$). The transition from area below the bistability area **C** to the resonance area **D**, caused by the additional exciting moment $\zeta_d(380-440 \text{ seconds}) = 0.013$.

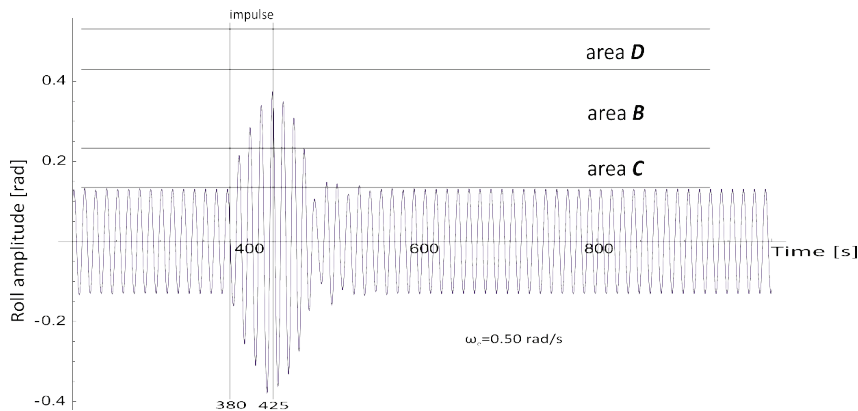


Fig. 5. Roll time history for the OSV vessel ($T = 6.10$ m, $GM_0 = 2.50$ m, $\zeta_w = 0.039$). The reaction to the additional exciting moment $\zeta_d(380-425 \text{ seconds}) = 0.013$

Cases when the excitation moment induces stable amplitude of rolling within the bistability area **C**

In Fig. 6 (left), the initial and stable roll amplitude is below but very close to the upper limit of the bistability area **C**. From the 450 second of simulation time the impulse in the form of additional excitation moment M_d is introduced. Its value is very small ($\zeta_d \approx 5\%$ of ζ_w) and duration time is short (5 seconds). The energy which is added to the system is small but big enough for entering area **B**. Entering area **B** is very shallow but sufficient for the transition (amplitude jump) to area **D** and next the appearance of stable resonant rolling. A similar situation is presented in Fig. 6 (right), where initial rolling is also in area **B**, however not so close to its upper limit. The only difference is that the value of the impulse ζ_d , needed to induce the shallow entry into area **B** must be bigger. In both cases crossing through area **B** takes place without any additional energy support – although it needs some oscillation cycles to fulfil.

Entering area **B** not always provides the transition. The transition also depends on the oscillation phase at which the additional exciting moment M_d occurs. In roll time history shown in Fig. 7 M_d occurs three times. Each time, its value and duration are the same as well as the direction is compatible with M_w . The only difference is the oscillation phase of its occurrence. Each time, the oscillations enter the area of unstable solution but only in the third case, the transition is observed.

Another, very interesting case is presented in Fig. 8, where the situation is similar to the one presented in Fig. 6 (right). The difference is that during the crossing the area **B**, from 600 to 615 seconds of simulation the additional impulse M_d is introduced – its direction of action is opposite to M_w . It can be seen that M_d enforces the decrease of the oscillations amplitude and the direction of its return to area **C**. However, when M_d is stopped the amplitude of oscillations strives to area **D** afresh.

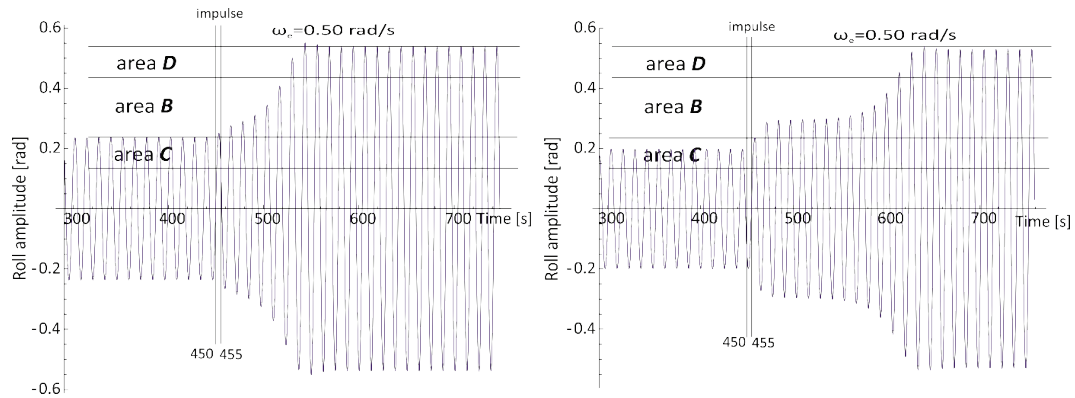


Fig. 6. Roll time history for the OSV vessel ($T = 6.10$ m, $GM_0 = 2.50$ m, $\zeta_{w,left} = 0.0498$, $\zeta_{w,right} = 0.0482$)
The transition from the bistability area C to the resonance area D, caused by the additional exciting moment $\zeta_d(450-455$ seconds)

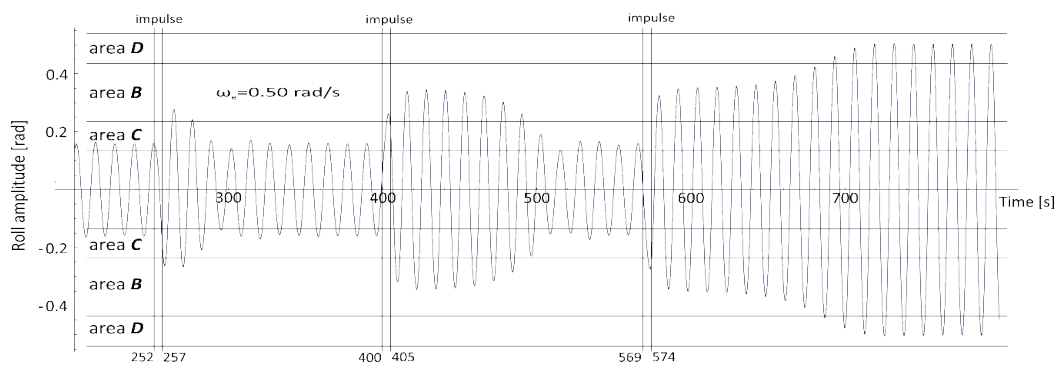


Fig. 7. Roll time history for the OSV vessel ($T = 6.10$ m, $GM_0 = 2.50$ m, $\zeta_w = 0.044$). The additional exciting moments: $\zeta_{d1}(252-257$ seconds) = $\zeta_{d2}(400-405$ seconds) = $\zeta_{d3}(569-574$ seconds) = 0.0345

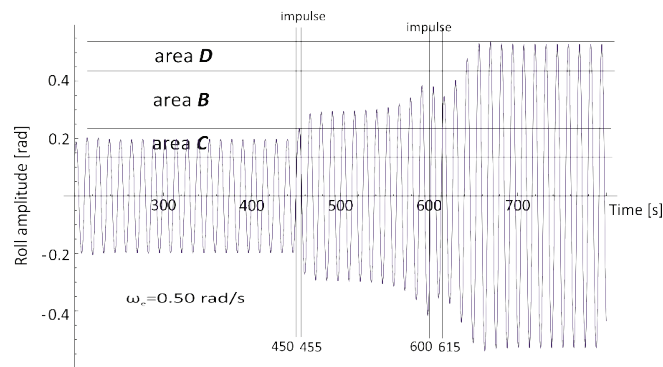


Fig. 8. Roll time history for the OSV vessel ($T = 6.10$ m, $GM_0 = 2.50$ m, $\zeta_w = 0.0482$). The additional exciting moments: $\zeta_{d1}(450-455$ seconds) = 0.015, $\zeta_{d2}(600-615$ seconds) = -0.015

5. Summary

The article presents a few scenarios of crossing of the area of the unstable solution of the roll equation for cases when strong nonlinear oscillations occur. Obviously, there are many scenarios that are more possible but the focused of this article has been narrowed for the purpose of presentation. Although, the main goal of this article was to show, only to some extent, the possible complexity of nonlinear rolling. The phenomena characteristic for nonlinear rolling can be observed most often when the maximum of the GZ curve is located at relatively small angles. For a ship that meets the intact stability criteria these angles are close to 25-35°. Given that extreme amplitudes of resonant rolling can achieve 35-40°, it should be assumed that nonlinear oscillations could occur under real conditions.

The rolling scenarios presented in the article show that under some circumstances rolling could be interpreted as chaotic. In such situations, rolling simulations performed with the use of linear or close to linear techniques can give incorrect information about the ships response to external extortion especially when irregular waves are considered. The possibility of the occurrence of chaotic rolling can be read from the roll spectrum only if it shows the bistability areas and area of unstable solution of roll equation. However, the analysis of ship rolling based on bistability areas, area of unstable solution is a new approach to rolling, and it requires further work.

It is very important to note that the presented analysis concerns the mathematical model of rolling and it has not been tested during ship model tests.

References

- [1] Bassler, C., Reed, A., *A method to model large amplitude ship roll damping*, Proceedings of the 11th International Ship Stability Workshop, pp. 217-224, 2010.
- [2] Falzarano, J., Taz Ul Mulk, M., *Large amplitude rolling motion of an ocean survey vessel*, Marine Technology, Vol. 31, pp. 278-285, 1994.
- [3] Fossen, T., Nijmeijer, H., (eds.), *Parametric resonance in dynamical systems*, Springer Science Business Media, LLC, http://dx.doi.org/10.1007/978_1-4614_1043-0, 2012.
- [4] Francescutto, A., Contento, G., *Bifurcations in ship rolling: experimental results and parameter identification technique*, Ocean Eng., Vol. 26, pp. 1095-1123, 1999.
- [5] Himeno, Y., *Prediction of ship roll damping – state of the art*, Report of Dept. of Naval Architecture and Marine Engineering, The University of Michigan, No. 239, 1981.
- [6] ITTC Recommended Procedures, *Numerical Estimation of Roll Damping*, ITTC, 2011.
- [7] Jordan, D. W., Smith, P., *Nonlinear ordinary differential equations – An introduction for scientists and engineers* (4th ed.), Oxford University, 2007.
- [8] Kawahara, Y., Maekawa, K., Ikeda, Y., *A simple prediction formula of roll damping of conventional cargo ships on the basis of Ikeda's method and its limitations*, Journal of Shipping and Ocean Engineering, Vol. 2, pp. 201-210, 2012.
- [9] Kiewrel, A., *Nieliniowy rezonans mechaniczny w modelach matematycznych maszyny synchronicznej*, Prace Naukowe Instytutu Maszyn, Napędów i Pomiarów Elektrycznych Politechniki Wrocławskiej, Nr 50, pp. 251-259, 2000.
- [10] Liangqiang, Z., Fangqi, Ch., *Stability and bifurcation analysis for a model of a nonlinear coupled pitch–roll ship*, Mathematics and Computers in Simulation, Vol. 79, pp. 149-166, 2008.
- [11] Wawrzyński, W., Krata, P., *On ship roll resonance frequency*, Ocean Eng., Vol. 126, pp. 92-114, 2016.
- [12] Wawrzyński, W., *Bistability and accompanying phenomena in the 1-DOF mathematical model of rolling*, Ocean Eng., Vol. 147, pp. 565-579, 2018.

Manuscript received 09 May 2018; approved for printing 17 August 2018